

## STEREOLOGICAL INVESTIGATION OF SPATIAL FIBRE PROCESSES USING CONFOCAL SCANNING LASER MICROSCOPY

Torsten Mattfeldt<sup>1</sup>, Ashley Clarke<sup>2</sup>, Geoff Archenhold<sup>2</sup>

<sup>1</sup> Department of Pathology, University of Ulm  
Oberer Eselsberg M23, D-89081 Ulm, Germany

<sup>2</sup> Molecular Physics and Instrumentation Group  
Department of Physics, University of Leeds  
GB-Leeds LS2 9JT, Great Britain

### ABSTRACT

A design-based stereological method is presented which enables the unbiased estimation of mean length per unit volume and of the angle distribution of spatial fibre processes from arbitrarily directed pairs of registered parallel optical sections. The theory is illustrated by an application where the directional distribution of glass fibres is monitored in a stepwise extruded polymer composite by the stereological evaluation of data obtained by confocal scanning laser microscopy.

**Keywords:** Anisotropy, confocal scanning laser microscopy, directional statistics, fibre processes, stereology, stochastic geometry.

### INTRODUCTION

Fibrous structures are sets of long, thin, smoothly curved or linear features, embedded in a three-dimensional matrix. When one abstracts from their thickness, they may be considered as *spatial fibre processes* (Stoyan et al., 1987, pp. 228–256). A fibre is a sufficiently smooth, continuously differentiable unoriented curve of finite length. A spatial fibre process is the union of fibres, arranged in an unbounded three-dimensional reference space according to some random mechanism. Let us consider ergodic stationary spatial fibre processes which are non-necessarily isotropic. In stereological studies on fibrous structures, estimation of the *intensity*  $L_V$  — mean length of fibres per unit reference volume — is of central importance. However, fibre processes with identical  $L_V$  may be arranged in an entirely different manner with regard to their spatial and angular distributions. The angle distribution created during processing controls important physical properties of *fibre-reinforced composites* (Clarke et al., 1993). We present a design-based approach which enables the unbiased estimation of  $L_V$  and of the angle distribution of non-necessarily isotropic fibre processes from arbitrarily directed pairs of registered parallel optical sections.

## MATHEMATICAL BACKGROUND

*Vectorial* directions (orientations) in space can be considered as "arrows" and may be represented as points on the surface of a sphere with radius 1, which we denote as  $\mathcal{S}$ . Orientations are thus given by a colatitude  $\theta \in [0, \pi]$  and a longitude  $\phi \in [0, 2\pi]$ . These angles are defined in a spherical polar coordinate system, where the  $z$ -axis coincides with the polar axis and the  $xy$ -plane is the equatorial plane. The colatitude is the angle between a direction and the  $z$ -axis, whereas the longitude is the angle between the projection of the direction onto the  $xy$ -plane and the  $x$ -axis, measured counterclockwise (Fig. 1). *Axial* directions can be viewed as directed, but unoriented lines in three-dimensional space and may be represented as points on the surface of a hemisphere with unit radius,  $\mathcal{H}$ . An axial direction may be defined by a colatitude  $\theta \in [0, \pi]$  and a longitude  $\phi \in [0, \pi]$ . Fibre processes have axial directions, but no orientations. The directional distribution of the process is given by the angle distribution of the tangents to the fibres at a *typical fibre point*. The latter may be considered as a point that is selected with uniform probability along all length elements of the fibres of the ergodic process. When planes intersect fibres, one obtains intersection points. A *typical intersection point* is obtained by uniform sampling of these intersection points. In general, a typical intersection point is not a typical fibre point, because the directional distribution of the tangents at a typical intersection point is weighted in proportion to  $|\cos \theta|$ . To explore the directional distribution of a fibre process, three steps are therefore necessary: (i) estimation of the fibre directions sampled at intersection points, (ii) estimation of the *true* angle distribution of the fibre process from the *observed* angle distribution as measured at intersection points, and (iii) a statistical analysis of the estimated true directional distribution of the fibres.

The angles  $\theta$  and  $\phi$  can be determined without shape assumptions when a set of registered serial sections is available. One follows the fibres in two (or more) closely neighbouring parallel physical or optical sections. It is necessary to know the distance  $\Delta z$  between the first plane and the final plane; let us denote these as the *reference plane* and the *look-up plane* (Sterio, 1984). The coordinates  $(x_1, y_1)$  and  $(x_2, y_2)$  of the intersection points, which the sampled fibres generate in the reference plane and in the look-up plane, respectively, are measured. Only those fibres are considered which intersect the reference plane inside the sampling frame. The angles  $\theta \in [0, \pi]$  and  $\phi \in [0, \pi]$  can be determined from the following equations:  $\tan \theta = \{(\Delta x)^2 + (\Delta y)^2\}^{1/2} / \Delta z$  if  $\Delta y \geq 0$  (Case I),  $\tan(\pi - \theta) = \{(\Delta x)^2 + (\Delta y)^2\}^{1/2} / \Delta z$  if  $\Delta y < 0$  (Case II), and  $\tan \phi = \Delta y / \Delta x$ , where  $\Delta x = x_2 - x_1$  and  $\Delta y = y_2 - y_1$  (Fig. 1; Clarke et al., 1993).

To estimate the true directional distribution of the fibre process, each pair of angles  $(\theta_i, \phi_i)$  must be weighted by  $w_i = 1/|\cos \theta_i|$  (Stoyan, 1984, 1985). We have an unbiased estimator of the intensity,  $\hat{L}_V$ :

$$\hat{L}_V = (1/A) \sum_{i=1}^N (1/|\cos \theta_i|) \quad (1)$$

where  $N$  = the number of fibre intersections in the sampling frame and  $A$  = area of the sampling frame in the reference plane;  $\theta_i$  is the  $\theta$ -angle at the  $i$ 'th intersection point. The sum of all weights  $W = \sum_{i=1}^N w_i$  is calculated, and the density function of the pairs of angles  $(\theta_i, \phi_i)$  is estimated for the primary sample and for the weighted sample. By classification into intervals of constant widths  $\Delta\theta = \pi/M$  from  $\theta = 0$  to  $\theta = \pi$ ,

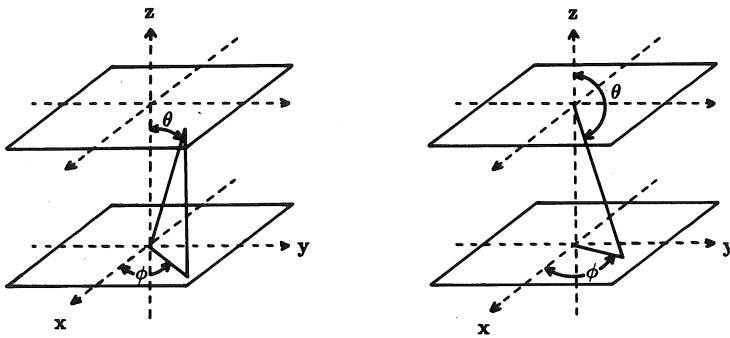


**Fig. 1.** Estimation of the angles  $\theta$  and  $\phi$  at intersection points. Below: reference plane with coordinates  $(x_1, y_1, z_1)$ , above: look-up plane with coordinates  $(x_2, y_2, z_2)$ . Left panel: Case I with  $y_2 > y_1$ ,  $0 \leq \theta \leq \pi/2$ . Right panel: Case II with  $y_2 < y_1$ ,  $\pi/2 \leq \theta \leq \pi$ .

numbered  $l \in [1, M]$ , and  $\Delta\phi = \pi/M$  from  $\phi = 0$  to  $\phi = \pi$ , numbered  $m \in [1, M]$ , the pairs of angles are grouped into  $M^2$  classes. In group  $(l, m)$  we find  $k_{lm}$  pairs of angles  $(\theta_i, \phi_i)$  with  $(l - 1)\Delta\theta < \theta_i \leq l\Delta\theta$ ,  $(m - 1)\Delta\phi < \phi_i \leq m\Delta\phi$ . The densities in the original sample are estimated by  $\hat{f}_{lm} = k_{lm}/(N\Delta\theta\Delta\phi)$ . To obtain the correctly weighted densities, the sum of weights  $w_i$  of the  $k_{lm}$  angles,  $W_{lm}$ , is calculated for each group. The corrected densities are then estimated according to  $f'_{lm} = W_{lm}/(W\Delta\theta\Delta\phi)$  and may now be compared with the probability density function (p.d.f.) of  $\theta$  and  $\phi$  at isotropy, i.e.  $f(\theta, \phi) = (2\pi)^{-1} \sin \theta$ .

Let us introduce the concept of *complete directional randomness* for uniformly and independently distributed directions (*CDR*). Vectors have the property of *CDR* if their orientations are distributed uniformly and independently on  $\mathcal{S}$ . Axial directions have this property if they are distributed uniformly and independently on  $\mathcal{H}$ . The *angular distance* on  $\mathcal{S}$  between two vectorial directions  $(\theta_i, \phi_i)$ ,  $(\theta_j, \phi_j)$  reads

$$\cos \alpha = \sin \theta_i \sin \theta_j \cos(\phi_i - \phi_j) + \cos \theta_i \cos \theta_j \tag{2}$$

Let us denote the cumulative distribution function (c.d.f.) of the  $N(N - 1)/2$  angular distances between all  $N$  different directions on  $\mathcal{S}$  by  $F(\alpha)$ . When  $N$  random points are independently and uniformly distributed on the surface of a sphere,  $F(\alpha)$  is the ratio of the area of a spherical cap, produced on  $\mathcal{S}$  by a cone with apex in  $(0, 0, 0)$  and semi-vertical angle  $\alpha$ , to the total area of  $\mathcal{S}$ . Thus we obtain

$$F(\alpha) = (1 - \cos \alpha)/2 = \sin^2(\alpha/2) \tag{3a}$$

By differentiation we obtain the p.d.f.  $f(\alpha)$  of the angular distances between all different orientations:

$$f(\alpha) = (1/2) \sin \alpha \tag{3b}$$

To determine the angular distance  $\beta$  between two *axial* directions, edge effects must be taken into account; note that  $0 \leq \beta \leq \pi/2$ . Consider two points  $A$  and  $B$  on  $\mathcal{H}$  and

place their *antipodes*  $A'$  and  $B'$  on the surface of the other hemisphere. The smaller one of the two angular distances  $AB = A'B'$  and  $AB' = A'B$  is the angle  $\beta$ . As the points  $A, B, A'$  and  $B'$  all lie on a common great circle, we have  $2AB + 2A'B = 2\pi$ , hence  $A'B = \pi - AB$ , and we obtain:

$$\beta = \alpha \quad \text{if } \alpha \leq \pi/2, \quad \beta = \pi - \alpha \quad \text{otherwise} \quad (4)$$

Using the same considerations as before, we obtain the desired results for  $CDR$  in the axial case:

$$F(\beta) = 1 - \cos \beta = 2 \sin^2(\beta/2) \quad (5a)$$

$$f(\beta) = \sin \beta \quad (5b)$$

A method to test a single sample of  $N$  equally weighted axial directions for  $CDR$  can be derived from eq. (5a). We calculate the  $N(N-1)/2$  angular distances  $\beta_{ij}$  between all different directions  $(\theta_i, \phi_i), (\theta_j, \phi_j)$ , then we use the sample c.d.f.  $\hat{F}(\beta)$  as an estimator of the c.d.f.  $F(\beta)$  of the process. In case of  $CDR$ ,  $\hat{F}(\beta)$  should not differ significantly from  $(1 - \cos \beta)$ . Acceptance regions for  $CDR$  can be obtained by Monte Carlo simulations. After appropriate weighting of the  $\beta_{ij}$  angles (see below), the same approach can also be used to test a spatial fibre process for  $CDR$  from samples of directions at intersection points. However, it should not be applied uncritically to arbitrarily small samples and to all kinds of fibre processes. If there are curved fibres, it happens with positive probability that a single fibre is intersected twice, but independent sampling of directions is necessary for the test. The effect should become negligible at large sample sizes, but the minimum required number of sample elements is not known. The test is correct if the curvature of the fibres is so small that (i) none of the fibres hits the sectional plane twice within the window of observation, and that (ii) changes of the local directions of the fibres from the reference plane to the look-up plane can be neglected at the selected distance  $\Delta z$ . These conditions always hold when the fibres are line pieces. The test should be safely applicable in large-sample studies on rather straight, rod-like fibrous structures; see the study on straight glass fibres below with several hundreds of measurements per sample as a model example.

In a stereological study where the fibre directions are measured at intersection points, we also first calculate the  $N(N-1)/2$  angular distances  $\beta_{ij}$  between all different directions  $(\theta_i, \phi_i), (\theta_j, \phi_j)$ . For the estimation of the sample c.d.f.  $\hat{F}(\beta)$ , however, each angular distance  $\beta_{ij}$  is weighted by  $w_{ij} = 1/(|\cos \theta_i| |\cos \theta_j|)$ . Again,  $\hat{F}(\beta)$  should not differ significantly from  $(1 - \cos \beta)$  at  $CDR$ . To analyze a set of  $N$  independently sampled directions, we perform simulations where  $N'$  primary points are thrown onto  $\mathcal{H}$  by inserting independent random numbers  $(x_1, x_2)$ , uniformly distributed within  $[0, 1]$ , into  $\phi = \pi x_1, \theta = \arccos(1 - 2x_2)$ . For each point, a third uniform random number  $x_3 \in [0, 1]$  is generated independently. Directions are only accepted for the secondary sample if  $|\cos \theta| > x_3$ . Thus the cutting process with sampling probability proportional to  $|\cos \theta|$  is simulated. The first  $N$  points of the secondary sample constitute the tertiary, final sample. As the mean number of secondary sample points is  $N'/2$  because of isotropy, but the number of directions varies between individual runs,  $N'$  should be distinctly larger than  $2N$ , e.g.  $N' \approx 2.5N$ . The c.d.f.  $F(\beta)$  is estimated for each simulation from the tertiary sample after weighting each angular distance  $\beta_{ij}$  by  $1/(|\cos \theta_i| |\cos \theta_j|)$ . By repeating the simulations, confidence regions for  $F(\beta)$  at  $CDR$  corresponding to any desired error probability with sample size  $N$  can be determined.

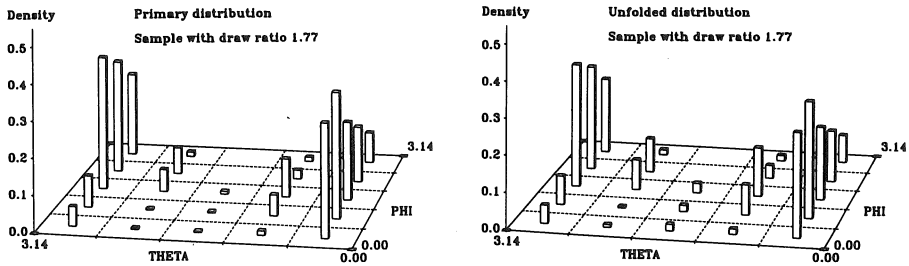


**Fig. 2.** Estimation ("unfolding") of the true angle distribution of the fibre process (right panel) from the angle distribution at the intersection points (left panel).

### EXAMPLE: DIRECTIONAL DISTRIBUTION OF GLASS FIBRES IN A POLYMER MATRIX

Glass fibre reinforced polyoxymethylene was studied in an initial state and after hydrostatic extrusion to increasing draw ratios  $\lambda$ . In short-fibre composites, these fibres may be considered as straight rods whose diameters are typically  $\approx 10 \mu\text{m}$ . The draw ratio is the final length of the billet in the draw direction, divided by the initial billet length. In addition to the initial billet where  $\lambda = 1$ , we studied 4 extruded samples with  $\lambda = 1.77$ , 3.65, 5.31, and 6.91 (Table I). Four transverse optical sections were used, i.e. the normal to the sections (= the  $z$ -axis) was taken parallel to the direction along which the samples were extruded, with a distance of  $5 \mu\text{m}$  apart from each other, hence  $\Delta z = 15 \mu\text{m}$ . A confocal scanning laser microscope BIORAD MRC 600 was used at  $60\times$  objective magnification at a laser wavelength of  $514 \text{ nm}$ . The final magnification at the level of the image analyzer was  $0.248 \mu\text{m}/\text{pixel}$ . The setting of the confocal pinhole was adjusted to obtain an optical thickness of  $1 \mu\text{m}$ . Fluorescence of the fibres was induced by chemical coating, and 36–50 non-overlapping rectangular counting frames of individual area  $191 \mu\text{m} \times 127 \mu\text{m}$  were taken along arbitrary diameter scans on the reference plane. For every sampled fibre, the coordinates of the intersection points  $(x_1, y_1)$  and  $(x_2, y_2)$  in the reference plane and in the look-up plane were recorded with an image analyzer. The angles  $(\theta_i, \phi_i)$  at the intersection points were determined with correction of a possible bias due to different refractive indices of immersion oil and the polymer matrix (Clarke et al., 1993). The next step was the estimation of  $L_V$  and of the "true" angular distribution by  $1/|\cos \theta_i|$ -weighting of the pairs of angles  $(\theta_i, \phi_i)$ , which were classified into  $M^2 = 25$  groups with constant widths  $\Delta\theta = \Delta\phi = \pi/5$  (Fig. 2). The function  $F(\beta)$  was estimated by  $1/(|\cos \theta_i| |\cos \theta_j|)$ -weighting. Thereafter 200 simulations with  $N' = 1200$  independent uniform random points on  $\mathcal{H}$  were performed. Secondary samples were obtained by giving each pair of angles  $(\theta_i, \phi_i)$  a chance of  $|\cos \theta_i|$  to survive. The tertiary samples consisted in the first  $N = 455$  directions of the secondary samples; this number was chosen because the *smallest* real sample of glass fibre directions had 455 elements (Table I). From each simulation, the function  $F(\beta)$  was computed, and the resulting values were ordered by size for each value of  $\beta$ . Thereafter, 99% confidence bands of  $F(\beta)$  for  $CDR$  corresponding to a sample size of  $N = 455$  were obtained by using the 2nd and the 199th of the ordered  $F(\beta)$ -values.

Table I

$\lambda$	$N$	$\hat{Q}_A$ [ $\frac{1}{\text{mm}^2}$ ]	$\hat{L}_V$ [ $\frac{\text{mm}}{\text{mm}^3}$ ]	$\hat{F}(\pi/4)$
1.00	455	659	990	0.472
1.77	626	516	590	0.732
3.65	780	699	713	0.986
5.31	552	455	463	0.997
6.91	797	699	712	0.995

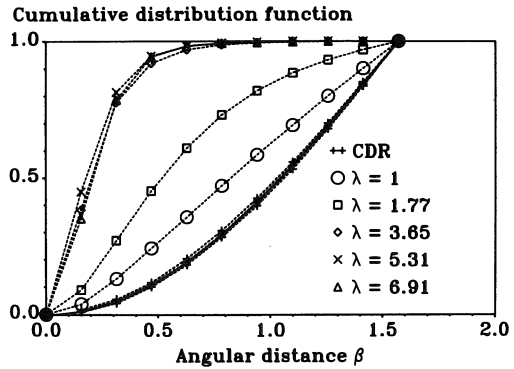


**Table I.** Results of the study on the glass-fibres reinforced composite.  $\lambda$ : draw ratio,  $N$ : number of measured directions per sample,  $\hat{Q}_A$ : estimated number of fibre intersections per unit reference area,  $\hat{L}_V$ : estimated mean length of glass fibres per unit reference volume,  $\hat{F}(\pi/4)$ : estimated probability that the angular distance  $\beta$  between the directions of two uniformly sampled length elements of the glass fibres is  $\leq \pi/4$ . **Fig. 3.** Estimates of  $F(\beta)$  at different draw ratios  $\lambda$  together with the mean values and the 99% confidence bands of  $F(\beta)$  at complete directional randomness (*CDR*), obtained by simulations based on a final number of  $N = 455$  sampled directions. Note increasing anisotropy with rising draw ratios, which produces clustered directions and thus rises the probability of small angular distances.

The effect of the weighting procedure is shown in Fig. 2. The densities in the lowest and highest class of  $\theta$  are lowered, and the densities in the middle range of  $\theta$  are raised. Table I and Fig. 3 show estimates of  $F(\beta)$  for different draw ratios together with the mean values and the 99% confidence band of  $F(\beta)$  at *CDR*, obtained from the simulations. The hypothesis of *CDR* is rejected for all samples. The estimates of  $F(\beta)$  are distinctly shifted towards the left, hence the directions are more strongly clustered than at *CDR*. One finds a distinct increase of anisotropy at  $\lambda = 1.77$  as compared to the unstretched sample. The other three samples are still more anisotropic, but the changes of  $\hat{F}(\beta)$  with increasing  $\lambda$  become smaller and smaller at very high draw ratios. The estimated p.d.f.s  $\hat{f}(\beta)$  (not displayed) lead to the same conclusion.

## REFERENCES

- Clarke A, Davidson N, Archenhold G. Measurements of fibre directions in reinforced polymer composites. *J Microsc* 1993; 171:69-79.
- Sterio DC. The unbiased estimation of number and sizes of arbitrary particles using the disector. *J Microsc* 1984; 134:127-136.
- Stoyan D. Further stereological formulae for spatial fibre processes. *Math Operationsforsch Statist [Ser Statist]* 1984; 15:421-428.
- Stoyan D. Stereological determination of orientations, second-order quantities and correlations for random spatial fibre systems. *Biometr J* 1985; 4:411-425.
- Stoyan D, Kendall WS, Mecke J. *Stochastic geometry and its applications*. Chichester: Wiley, 1987.